International Journal of Thermophysics, Vol. 2, No. 4, 1981

Near Infrared Absorption Coefficient of Molten Glass by Emission Spectroscopy

J. I. Berg[1]

Received May 6, 1981

Emission spectroscopy is applied in the determination of the near infrared spectral absorption coefficient of molten glass. The glass is held in a small horizontal platinum alloy crucible, within an electrically heated cell, optically coupled to a Fourier transform spectrometer. A formula is derived which relates emissivity to absorption coefficient, thickness, and reflectivities for the glass-air and glass-metal interfaces. The reflectivity parameters are determined, in effect, by varying the thickness. Spectral absorption coefficient results are compared with results of transmission spectroscopy. The emission technique is advantageous in that it eliminates the problem of chemical reactions with window materials used in the transmission method, and sample preparation and interfacing to commercially available spectrometers is simplified.

KEY WORDS: Fourier transform spectroscopy; infrared properties of glass; semitransparent materials; spectral absorption coefficients; spectral emissivity.

1. INTRODUCTION

In transparent or semitransparent materials, radiation is emitted omnidirectionally from each volume element within the sample, and the emission and propagation laws must be used to determine the distribution of externally emitted radiation. Only when the absorption coefficient is much larger than the reciprocal of the smallest sample dimension is it correct to use the opaque body approximation, with emission becoming a surface phenomenon.

Molten glasses which have been fused from silica and other oxides at high temperatures are semitransparent materials. During the melting and much of the forming processes, heat is transferred largely by emission and absorption of radiation. It is primarily the glass absorption coefficient

[1] Research and Development Division, Owens-Corning Fiberglass Corporation, Technical Center, Granville, Ohio 43023, USA.

0195-928X/81/1200-0381$03.00/0

which controls this energy exchange. This paper describes a newly developed technique for determination of the spectral absorption coefficient from the emission spectra of layers of glass at molten state temperatures. The technique could be applied to other semitransparent liquids over a wide temperature range, and the concepts are applicable to solids as well.

Numerous investigators have reported on absorption coefficient determination by transmission of radiation through molten glass held between transparent windows made of silica or sapphire [1–5]. In emission, molten glass is held in open, horizontal crucibles. This eliminates the problem of chemical reactions with window materials used in transmission and simplifies sample preparation. Optical interfacing to a spectrometer is somewhat simpler in that radiation is not directed toward the sample, only from it to the spectrometer. Finally, the problem of separating sample self-radiation from spectrometer source radiation is completely eliminated, since the sample and spectrometer radiation source are the same. Use with a high-speed Fourier transform spectrometer has allowed the recording of several complete spectra during oxidation-reduction reactions within the glass [6].

An interesting new technique reported recently by Ades and Traverse [7] eliminates some of the objections to the transmission approach. By using a tunable laser, these investigators have performed transmission measurements on very small regions of glass supported by surface tension, thus avoiding contact of any material with the region of glass studied.

Emission spectroscopy has been used in certain applications to obtain absorption information, and progress in this area has been reviewed by Huong [8]. Absorption coefficient values obtained by emission have been reported by Kozlowski [9] and Wilmhurst [10] for molten salts and by Dvurechensky et al. [11] on silica glass. The main emphasis in the present paper is in establishing the validity of the emission technique and addressing problems associated with its use. It is profitable in the first respect to review basic emission principles, arriving at a more complete and concise expression relating emissivity and absorption coefficient. Results for different sample thicknesses are compared in order to check the formula and its use. An independent check on the technique is provided by comparison with results from a transmission method for the same composition and temperature. Finally, attention is given to the optical role of the backplate supporting the liquid layer, the elimination of unwanted radiation, and the requirements on the reference used in measuring emissivity.

2. RELATIONSHIP BETWEEN EMISSIVITY AND ABSORPTION COEFFICIENT

The emissivity factor is defined as the ratio of sample radiance to that of a blackbody emitter under the same conditions of temperature and

geometry. In the present discussion, the term applies to radiation emitted within a cone of very small solid angle near the normal to a surface of opaque material or to a layer of semitransparent material.

The layer emissivity formula is derived here from two apparently distinct starting points. However, it should be recognized that both derivations rest on the energy balance principle. The first derivation is based on the bulk media statement of energy balance and the second on that applied to the space inside a blackbody cavity.

2.1. Derivation from Bulk Emissive Power

In an isotropic medium, radiation is emitted from each small element omnidirectionally. The spectral volume emissive power, $J(\lambda, T)$, is the radiant power emitted at wavelength λ by a unit volume at temperature T into a unit solid angle, per unit wavelength interval. This is expressed using the more familiar blackbody hemispherical radiant flux density, $W_B(\lambda, T)$, by the formula [12, 13]

$$J(\lambda, T) = \alpha(\lambda, T)n^2(\lambda, T)W_B(\lambda, T)/\pi \tag{1}$$

Here α is the spectral absorption coefficient, and n is the spectral index of refraction of the material.

Since internal absorption is also controlled by α, this process introduces no additional parameters. Referring to Fig. 1, the free surface reflectivity, R_1, depends on n through Fresnel's equation:

$$R_1 = (1 - n)^2/(1 + n)^2 \tag{2}$$

Reflection from the backplate, however, is controlled by the physical nature of the interface, so that R_2 is an additional parameter. This may be related to the emissivity into the glass by Kirchhoff's law and considerations of equilibrium thermal radiation in a dielectric medium [12]:

$$\epsilon_2 = (1 - R_2)n^2 \tag{3}$$

The emissivity is thus characterized by three optical parameters, including α. Thus, the determination of α requires emissivity determinations for three separate thicknesses, L. Since each emissivity is a ratio of radiances for the respective thickness to that of a common blackbody emitter, four separate spectra are actually required. However, this number may be decreased, in practice, if one or more of the parameters do not vary with temperature, wavelength, or ranges of chemical composition.

In deriving the expression for emissivity in terms of α, L, R_1, and R_2, it is convenient initially to ignore the effect of the glass-air interface in

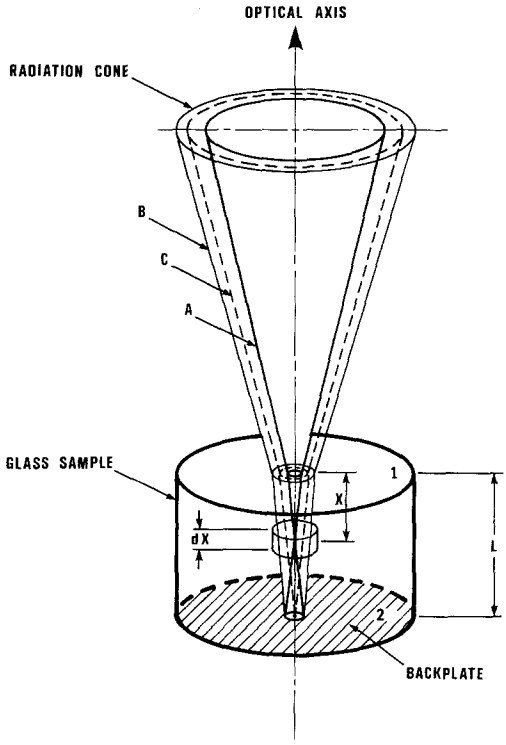

Fig. 1. Illustration of the three primary components of emitted radiation: (A) Radiation from an internal point emitted in the forward direction, (B) radiation from an internal point emitted in the backward direction and reflected forward by the backplate, and (C) radiation emitted forward by the backplate. The glass-air and glass-backplate interfaces are numbered 1 and 2, respectively, in correspondence with the text.

reflecting radiation, but to include its refracting effect. Refraction causes cancellation of the n^2 in Eqs. (1) and (3), since the solid angle becomes multiplied by n^2, and the intensity is therefore divided by n^2. This is illustrated in Fig. 1 for $n > 1$. Denoting this internal emissivity by e, the forward contribution from a layer of thickness dx at depth x, from Eq. (1) and the exponential absorption law, is

$$de = \alpha \exp(-\alpha x)\, dx \tag{4}$$

since the forward blackbody radiance is W_B/π. An equal amount of radiation is emitted backward, and this is partially reflected forward by the backplate. Also, the backplate itself emits. The three separate contributions

illustrated in Fig. 1, integrated over x from zero to L are

$$e_A = 1 - \exp(-\alpha L) \tag{5a}$$

$$e_B = R_2\left[\exp(-\alpha L) - \exp(-2\alpha L)\right] \tag{5b}$$

$$e_C = (1 - R_2)\exp(-\alpha L) \tag{5c}$$

The net internal emissivity is then

$$e = e_A + e_B + e_C = 1 - R_2\exp(-2\alpha L) \tag{6}$$

As mentioned, Eq. (6) is already corrected for refraction. Reflection decreases the forward intensity by $(1 - R_1)$, but the reflected radiation can undergo an infinite number of internal reflections. This is expressed mathematically as an infinite geometric series. The net external emissivity, from Eq. (6), is

$$\epsilon = (1 - R_1)(1 - R_2\exp(-2\alpha L))/\left[1 - R_1R_2\exp(-2\alpha L)\right] \tag{7}$$

where the denominator in Eq. (7) is the closed form summation of the infinite series.

This exact result is actually of a more simple form than the approximations which have appeared [8,9]. Since it contains only terms in $\exp(-2\alpha L)$, it may be inverted to yield

$$\alpha = (1/2L)\ln\left[R_2(1 - \epsilon R_1/(1 - R_1))/(1 - \epsilon/(1 - R_1))\right] \tag{8}$$

A modified form of Eq. (8) (see Section 2.3) is used in obtaining the absorption coefficient from emissivity.

2.2. Derivation from Kirchhoff's Law

For the present purpose, the sample is considered to be a part of an internal wall of a blackbody cavity. A cone with apex on the wall, oriented near the normal, contains some radiation emitted from the sample, some reflected from a similar cone on the opposite side of the normal, and some incident cavity radiation. Energy balance (Kirchhoff's law) demands that

$$\epsilon + r = 1 \tag{9}$$

where r is the sample normal reflectivity.

The reflectivity contains a component R_1 from the surface and a term arising from the backplate. Only the second is subject to multiple internal

reflection, giving

$$r = R_1 + R_2(1 - R_1)^2\exp(-2\alpha L)/(1 - R_1R_2\exp(-2\alpha L)) \quad (10)$$

From Eqs. (9) and (10), an expression identical to Eq. (7) results.

2.3. Absorption Coefficient in Terms of Emissivity Ratios

The emissivities in the optically thick ($\alpha L \gg 1$) and optically thin ($\alpha L \ll 1$) limits, from Eq. (7), are

$$\epsilon_\infty = 1 - R_1 \quad (11a)$$

$$\epsilon_0 = (1 - R_1)(1 - R_2)/(1 - R_1R_2) \quad (11b)$$

ϵ_∞ and ϵ_0 are the maximum and minimum emissivities, respectively. Since the quantity $(1 - R_1)$ can be factored from Eq. (7), it is convenient to use the ratios of actual to maximum emissivities. However, R_1 still appears because of the internal reflection correction. Using Eq. (11b) to eliminate $(1 - R_1)$, Eq. (8) becomes

$$\alpha = (1/2L)\big[\ln((1 - \epsilon_0/\epsilon_\infty)/(1 - \epsilon/\epsilon_\infty)) + \ln((1 - R_1\epsilon/\epsilon_\infty)/(1 - R_1\epsilon_0/\epsilon_\infty))\big] \quad (12)$$

Only the second term in brackets in Eq. (12) is influenced by internal reflection, and therefore internal reflection results in an additive correction in the absorption coefficient determination. Expansion of the logarithmic functions indicates that the correction is smaller than the uncorrected portion by about the factor R_1.

3. EXPERIMENTAL APPARATUS AND TECHNIQUE

The high temperature cell illustrated in Fig. 2 was constructed in an effort to surround the sample with radiating regions at the same temperature, yet allow some pure sample radiation to emerge. Tradeoffs had to be made between these two conflicting requirements, and it was particularly difficult to eliminate radiation emitted from the cell top and reflected by the crucible bottom, as discussed below.

The cell was electrically heated by an ac current flowing through the inner cell wall and side pieces, made of a 75% Pt-25% Rh alloy. Brass electrodes, to which the side pieces were clamped, also served to hold the cell in place. The refractory pedestal could be lowered for sample insertion.

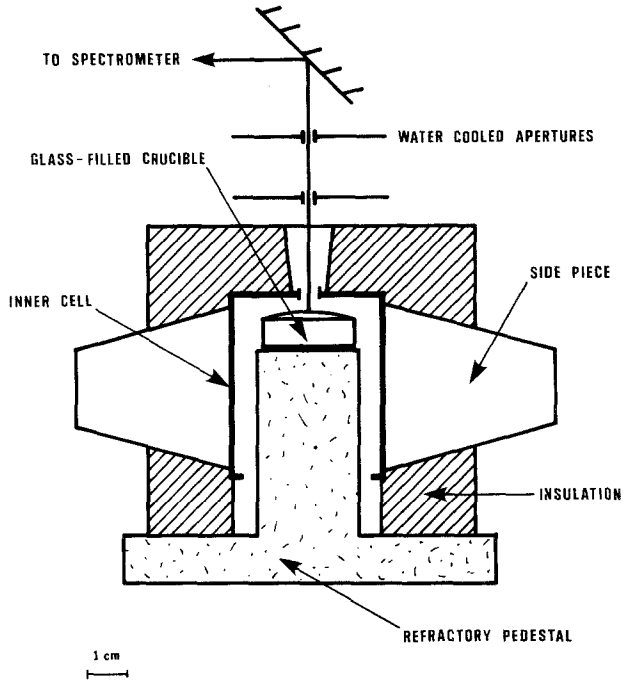

Fig. 2. The high temperature emission cell and apertures.

For improved heat dissipation and temperature uniformity, the cylindrical wall was constructed from three cylindrical bands of differing material thicknesses, each 12.7 mm in height. Thermocouples were welded to each band and to the top. Net temperature differences from top to bottom of 15°C could not be avoided. On the basis of a graybody approximation, the average temperature gradient of about 3 deg/cm magnitude would result in about a 1% error in the emissivity. This follows from addition of a term $\partial e/\partial x = (3/T)(dT/dx)$ to α in Eq. (4).

The cooled apertures above the cell were much smaller in diameter than the cell opening. This helped to eliminate radiation from the cell top. In order to eliminate reflected cell top radiation, the crucible bottom had to be highly polished and oriented normal to the optical axis defined by the outer apertures. The orientation was accomplished by lowering the pedestal slightly and orienting the pedestal support for minimum signal, using a polished disk in place of the sample. A similar procedure, with the pedestal removed completely, was used in centering the cell with respect to the axis. For elimination of reflected radiation, the crucible bottom had to be flat or slightly concave, while the (upper) glass surface had to be flat or slightly

convex. This latter condition required the crucible to be filled or slightly overfilled. Therefore, glass thickness could be changed appreciably only through use of crucibles of varying heights.

Placement of a sufficiently roughened or nonoriented sample on the pedestal yielded nearly the same signal, independently of sample details, to a few percent. This was taken as an indication that blackbody conditions were approximated to within a few percent. This signal was therefore used as a blackbody reference in emissivity experiments, so that no separate blackbody reference was required. The pedestal top itself, when sufficiently roughened, served the purpose well.

The spectrometer used in the measurements was a Digilab FTS-15B Fourier transform spectrometer, equipped for the near infrared. An auxiliary optical system mounted on the source end of the spectrometer console directed the radiation emitted vertically from the cell into the horizontal plane of the spectrometer and focused it on the iris of the emission attachment supplied by the manufacturer. The spectrometer recorded a complete spectrum in less than 1 s. However, the order of 100 scans had to be taken and signal-averaged in order to obtain an acceptable signal to noise ratio.

4. EXPERIMENTAL RESULTS ON GLASSES

Calcium-aluminum borosilicate glasses, prepared as discussed in ref. [6], were studied in the spectral region from 1 to as high as 5 μm. The glasses are sufficiently transparent for spectroscopic studies below about 3.5 μm. Small amounts of iron in the ferrous (Fe^{2+}) state give rise to room temperature bands peaking at 1.1 and 1.8 μm, while hydroxyl groups cause a band at 2.7 μm. These features are apparent also at elevated temperatures, although sufficient spreading occurs to obscure the weaker 1.8 μm peak.

In Figs. 3 and 4, spectral emissivities are shown for varying ferrous iron contents (here supported as weight percent FeO) and layer thicknesses. Also shown in Fig. 3 is the emissivity of the metal crucible bottom. Increasing noise occurring at shorter wavelengths, below the blackbody peak of about 1.9 μm, is indicated by a split in the curves, with the separation equal to the rms noise value.

Above about 4 μm (shown only in Fig. 4), all samples are opaque, and the emissivity approaches ϵ_∞. Emissivity increases with thickness and with the absorption coefficient, and thus with the FeO concentration. Therefore, the separation from the optically thick value occurs at longer wavelengths for thinner and more transparent samples.

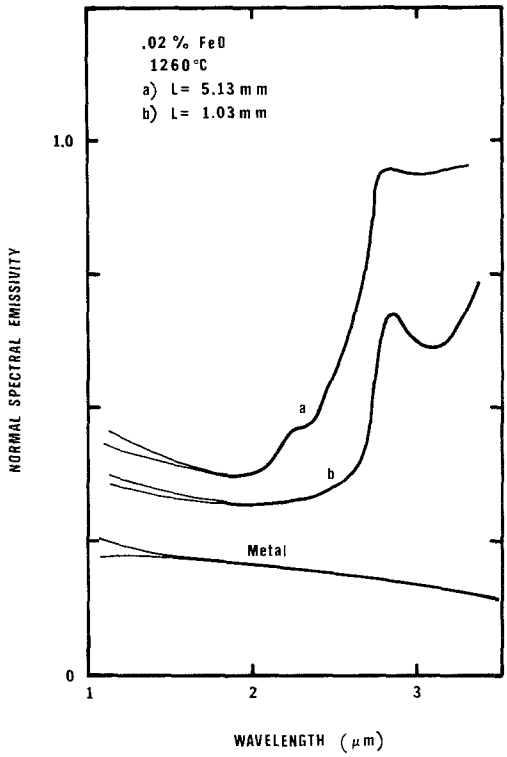

Fig. 3. Emissivities for low-iron glass layers of two thicknesses, L, and the emissivity of the metal crucible bottom. The separations in the curves at shorter wavelengths represent noise ranges, as discussed in the text.

To calculate the absorption coefficient, using Eq. (12), it is necessary to know the limiting emissivities, ϵ_∞ and ϵ_0. The index of refraction for most silicate glasses in the visible is near 1.5, giving $R_1 = 0.04$ by Eq. (2), or $\epsilon_\infty = 0.96$ by Eq. (11a). R_1 changes little over the near infrared region, and thus it is reasonable to take ϵ_∞ as a constant. Rather than take it equal to 0.96, however, it is expeditious instead to use the measured emissivity in the long wavelength limit for each sample. This compensates for any constant multiplicative error arising, for example, from spectrometer instability. Furthermore, it is then only required that the reference be a graybody, not necessarily a blackbody.

In the glass emissivity experiments, it was not possible to reach the optically thin limit. Because of surface tension and contact angle effects, it was not possible to obtain layers thinner than about 1 mm. Even glasses

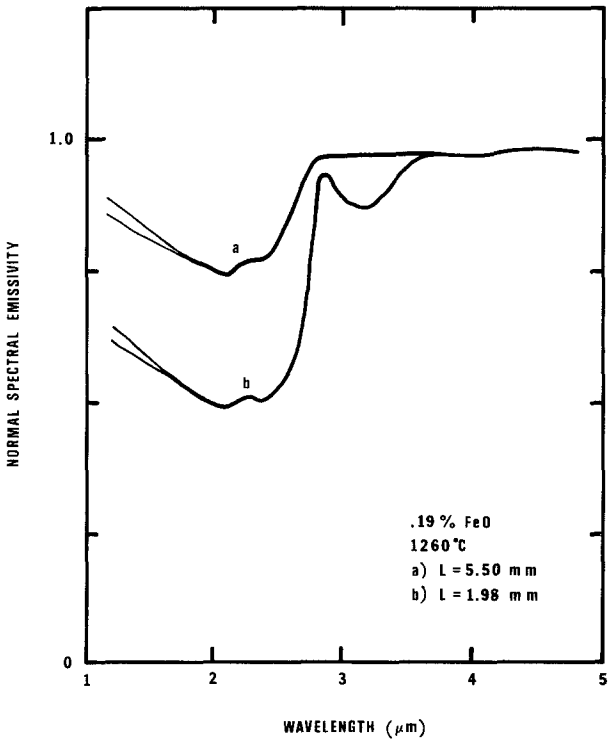

Fig. 4. Emissivities for a glass of a higher iron content.

melted from chemically pure oxides, with no deliberate iron addition, showed some absorption at this thickness. While ϵ_0 should not vary with the very small iron additions used, the crucible bottom emissivity was found to be sensitive to the surface preparation and thus varied from one crucible to the next. Since it was necessary to repolish the surfaces after removing glass with hydrofluoric acid, spectral measurements to determine ϵ_0 for each separate emissivity determination were necessary.

By applying the complex (wave) form of the Fresnel reflectivity law to the interface between a free-electron metal [14] and a dielectric of real index of refraction n, it is found that

$$1 - R_2 = n\epsilon_m \tag{13}$$

where ϵ_m is the emissivity of the metal into a vacuum. Thus, from Eq. (11b),

$$\epsilon_0 = \left[(1 - R_1)/(1 - R_1R_2)\right]n\epsilon_m \equiv \eta\epsilon_m \tag{14}$$

where Eq. (14) defines a parameter η of value slightly less than n. This, in what follows, is to be regarded as an empirical quantity.

The quantity η was further taken to be constant, independent of the crucible used and of wavelength. It was determined under the requirement that both emissivity curves of Fig. 3 give the same absorption coefficient by Eq. (12) over an intermediate wavelength range near 2 μm. Figure 5 shows the absorption coefficient calculated from Eqs. (12) and (14) with $\eta = 1.44$, somewhat less than the room temperature, visible index of refraction value of 1.56 for this glass. Considering the effects of wavelength and temperature, this value is reasonable. The discrepancy in absorption coefficient at longer wavelengths is understandable, since the emissivities very near 1.0, occurring for the thicker sample, cannot be used reliably in calculation. The same value of η was used for the higher iron glass of Fig. 4, with results shown in Fig. 6. In cases where there were discrepancies between samples,

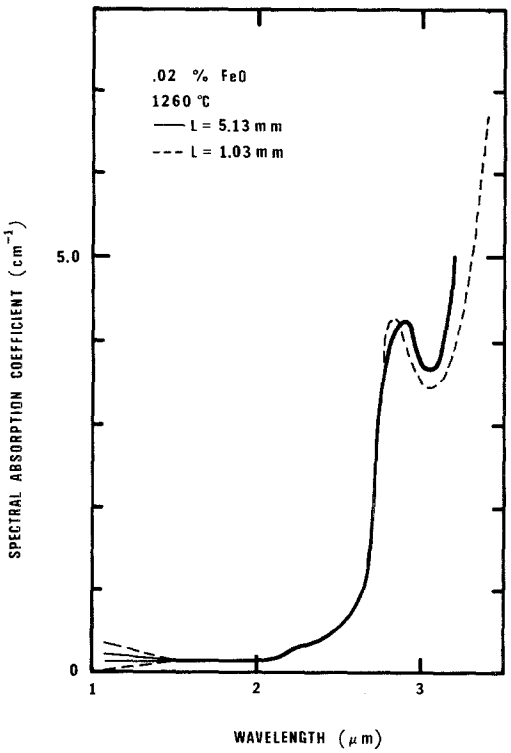

Fig. 5. Absorption coefficients calculated for the two thicknesses of Fig. 3 for the low-iron glass.

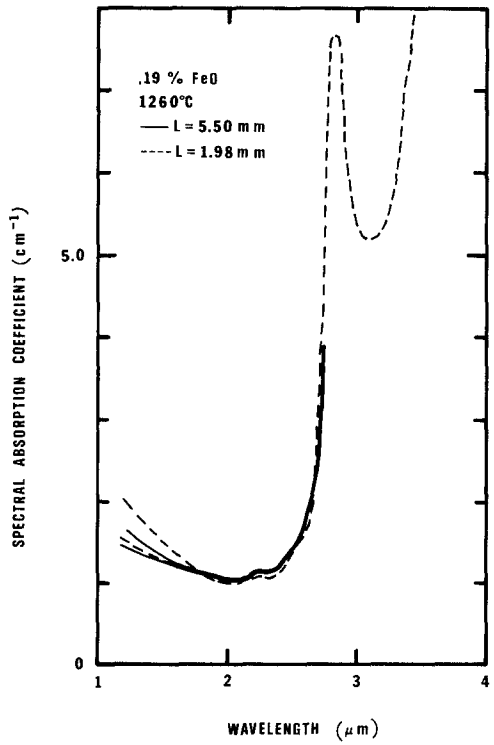

Fig. 6. Absorption coefficients calculated from data of Fig. 4 for the higher iron-containing glass.

thin sample emissivities were used at longer wavelengths, and thicker sample values were used at shorter wavelengths.

The wavelength dependence of the metal emissivity shown in Fig. 3 is similar to that reported by Maki et al. [15] for pure platinum, except that the magnitude is slightly higher. This may be because of surface roughness, a small amount of reflected radiation, or a higher alloy electrical resistivity than for pure Pt. Crucible bottom emissivities higher than normal could always be correlated with a high degree of surface roughness, curvature, or misorientation, and this check was made before proceeding to determine the absorption coefficient.

The parameter η was chosen to give agreement in α at 2.0 μm. However, agreement over an extended wavelength region is a legitimate test of the technique. As an independent check, a sample was submitted for transmission measurements to D. W. Johnson of Pilkington Brothers, Ltd.,

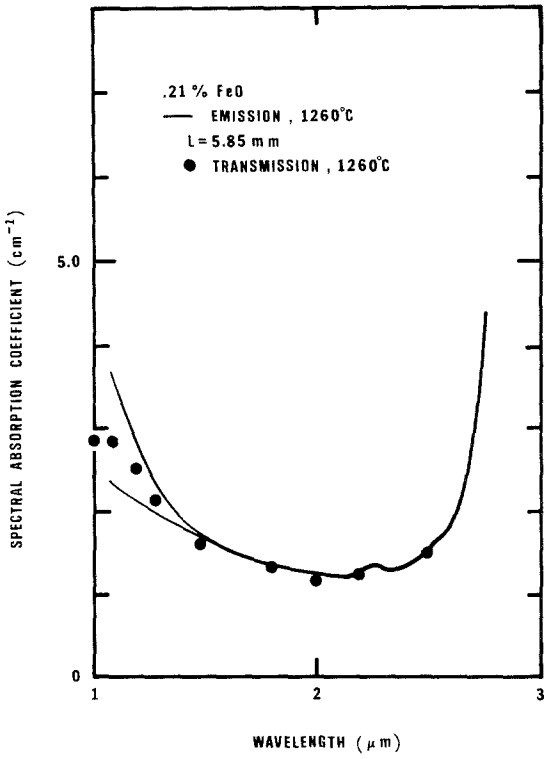

Fig. 7. Comparison of absorption coefficients determined by emission and transmission methods (transmission measurements by D. W. Johnson of Pilkington Brothers, Ltd.).

Research Laboratories, Lathom, England. Silica windows were used in a cell similar to that described earlier [13]. The results are shown in Fig. 7. Within the noise limits, the agreement is very good. Clearly, improvement in the short wavelength response of the spectrometer would improve the accuracy of the emission method.

The absorption coefficient values presented here were measured within 10 min of heating the glass from room temperature (3 min equilibration and 7 min scanning time). As discussed in ref. [6], oxidation of the glass results in conversion of iron from the ferrous to the ferric state at high enough rates that spectroscopic results on molten glass can be influenced. The spectrum taken immediately upon heating varies negligibly over the range 1040 to 1425°C. The room temperature spectrum [6] shows only minor differences from the high temperature spectrum. It has also been

reported [6] that the initial absorption intensity is directly proportional to the chemically analyzed ferrous iron content.

5. ACKNOWLEDGMENTS

The high temperature emission cell was designed and tested by C. L. McKinnis, and credit for recognition of the advantages and potential of the emission technique for molten glass studies belongs to him. The author would like to thank T. C. Welsh, who took most of the emission data, D. S. Goldman, who critically evaluated the emission technique, and D. W. Johnson of Pilkington Brothers, Ltd., who performed the high temperature transmission measurements. The encouragement of T. D. Erickson, W. W. Wolf, and R. T. Flynn is appreciatecd.

REFERENCES

1. L. Genzel, *Glastechn. Ber.* **24**:55 (1951).
2. F. J. Grove and P. E. Jellyman, *J. Soc. Glass Technol.* **39**:3 (1955).
3. M. Coenen, *Glastechn. Ber.* **41**(1):1 (1968).
4. B. Wedding, *J. Am. Ceram. Soc.* **58**:102 (1975).
5. V. A. Blazek, J. Endrys, J. Kada, and J. Stanek, *Glastechn. Ber.* **49**:75 (1976).
6. D. S. Goldman and J. I. Berg, *J. Noncryst. Solids* **38** & **39**:183 (1980).
7. C. Ades and J. P. Traverse, *J. Noncryst. Solids* **38** & **39**:257 (1980).
8. P. V. Huong, in *Advances in Infrared and Raman Spectroscopy*, Vol. 4, R. J. A. Clark and R. E. Hester, eds. (Heyden & Son, London, 1978), p. 85.
9. T. R. Kozlowski, *Appl. Opt.* **7**:795 (1968).
10. J. K. Wilmhurst, *J. Chem. Phys.* **39**:2545 (1963).
11. A. V. Dvurechensky, V. A. Petrov, and V. Yu. Reznik, *Infrared Phys.* **19**:465 (1979).
12. E. U. Condon, *J. Quant. Spectrosc. Radiat. Transfer* **8**:369 (1968).
13. R. Gardon, *J. Am. Ceram. Soc.* **39**:278 (1956).
14. J. M. Ziman, *Principles of the Theory of Solids* (Cambridge University Press, London, 1964), p. 237.
15. A. G. Maki, R. Stair, and R. G. Johnston, *J. Res. Natl. Bur. Standards* **64C**:99 (1960).